

# Orientation dynamics of weakly Brownian particles in periodic viscous flows

Piero Olla

*ISAC-CNR, Sez. Lecce, I-73100 Lecce, Italy.*

(Dated: November 23, 2018)

Evolution equations for the orientation distribution of axisymmetric particles in periodic flows are derived in the regime of small but non-zero Brownian rotations. The equations are based on a multiple time scale approach that allows fast computation of the relaxation processes leading to statistical equilibrium. The approach has been applied to the calculation of the effective viscosity of a thin disk suspension in an oscillating strain flow.

PACS numbers: 82.70.Kj, 47.15.Pn, 05.40.Jc, 92.10.Rw

## I. INTRODUCTION

The rheological properties of a suspension will depend, when the particles are non-spherical, on the orientation taken by the particles in response to the external flow. For a few particle shapes (e.g. the case of the ellipsoid [1]), equations for the rotation dynamics exist in closed form, and it is possible to determine the orientation distribution of the particles in suspension. However, unless a mechanism for the achievement of a statistical equilibrium is introduced, the orientation distribution will depend on the state in which the suspension is prepared initially. In the case of microscopic particles, one such mechanism is provided by Brownian rotations [2]. It is still unclear whether inertia and interaction with other particles may contribute to the equilibration mechanism.

An equilibrium distribution could be achieved alternatively by the presence of chaos in the rotation dynamics; unfortunately, the importance of chaos turns out to be small in most situations. In the case of a simple shear and axisymmetric particles, the particle motion is periodic [1]. This motion becomes aperiodic in the case of a time-dependent flow, but remains non-chaotic for axisymmetric particles [3]. Chaos arises in the motion of a triaxial ellipsoids in a simple shear [4], but, depending on the axis ratios, large domains of initial conditions remain associated with regular orbits and to the absence of a uniquely defined equilibrium distribution. Furthermore, for weak Brownian motion, the regular regions will act as attractors for the chaotic orbits and will provide the bulk of the orientation distribution.

The equilibrium orientation distribution of a Brownian particle has been determined in various important limit regimes, depending on the value of the Peclet number  $Pe$ , defined as the ratio of the velocity gradient and the angular diffusivity (which has the dimension of a frequency). The case of strong Brownian rotation was considered by Burgers [5] leading to an orientation distribution that in first approximation can be considered isotropic. A systematic perturbation theory in powers of  $Pe$  was introduced in [6], allowing the calculation of the effective viscosity of dilute suspensions, for values of  $Pe$  up to  $20 - 30$  [7].

More interesting is the case of weak Brownian motion, in which the form of the equilibrium distribution is determined by the structure of the orbits in orientation space, which in turn depends on the imposed flow. A technique for the determination of the equilibrium distribution of weakly Brownian particles, based on singular perturbation analysis of the diffusion equation in orientation space, was derived in [8] for the case of axisymmetric particles in a simple shear.

In the present paper, an alternative approach will be presented, based on the perturbative determination of the orbits in orientation space. This approach will appear to be appropriate in the case the flow is time-dependent, and, more in general, when analytical expressions for the unperturbed orbits are not available. For the sake of definiteness, the dynamics of a small disk in the field of an oscillating strain flow will be analyzed, and its contribution to the medium effective viscosity determined. This kind of flow could be obtained by means of a four-roll mill, as described in [3]; more interestingly, as it will be illustrated in the next section, an oscillating pure strain is what is seen by a particle in the velocity field of a gravity wave. This turns out to have application to models of wave propagation in polar seas. In fact, under cold and windy conditions, high concentrations of millimeter size ice crystals, called frazil ice, are generated in the water, modifying the medium viscosity and leading to increased wave damping [9, 10]. (Given the crystal size,  $Pe$  is in this case typically very large).

This paper is organized as follows. In the next section the orientation dynamics of a small disk will be analyzed in the absence of Brownian rotations. In Section III, the diffusion and drift across orbits in orientation space, produced by a weak noise, will be calculated perturbatively. In Section IV the results will be applied to the calculation of the effective viscosity of a dilute small disk suspension. Section V is devoted to conclusions.

## II. UNPERTURBED ORIENTATION DYNAMICS

Consider the motion of a particle in a velocity field  $\mathbf{U} = (U_1, U_2, 0)$ , which, at the particle position, has zero

vorticity, and strain  $\mathbf{E} = [\nabla\mathbf{U} + (\nabla\mathbf{U})^T]/2$  with components in the directions  $x_1$  and  $x_2$ :

$$\mathbf{E} = e \begin{pmatrix} (1 + \alpha) \cos \omega t, & (1 - \alpha) \sin \omega t \\ (1 - \alpha) \sin \omega t, & -(1 + \alpha) \cos \omega t \end{pmatrix}. \quad (1)$$

The interest in Eq. (1) is that it describes what is experienced by a fluid element in a gravity wave. In fact, the velocity field of a small amplitude gravity wave, would read, choosing the  $x_2$  axis pointing downward from the unperturbed water surface at  $x_2 = 0$  [11]:

$$\begin{aligned} U_1 &= \tilde{U} [e^{-kx_2} + e^{k(x_2-2h)}] \sin(kx_1 - \omega t), \\ U_2 &= \tilde{U} [e^{-kx_2} - e^{k(x_2-2h)}] \cos(kx_1 - \omega t), \end{aligned} \quad (2)$$

where  $h$  is the water depth. From the potential nature of the flow, the vorticity of the flow  $\mathbf{\Omega} = [\nabla\mathbf{U} - (\nabla\mathbf{U})^T]/2$  is zero and the strain at the sea surface  $x_2 = 0$ , has the form given by Eq. (1), with  $e = k\tilde{U}$ ,  $\alpha = \exp(-2kh)$ , and an initial phase different from zero for  $x_1 \neq 0$ . For small wave amplitudes, the displacement of a particle initially at the water surface will be small and the strain field experienced  $\mathbf{E}(\mathbf{x}(t), t) \simeq \mathbf{E}(\mathbf{x}(0), t)$  will be given by Eq. (1). Expressions for the strain field in the form of Eq. (1) can be shown to occur also for  $h \rightarrow \infty$ , from the superposition of progressive and regressive waves, with  $e = k\tilde{U}^+ > k\tilde{U}^-$ ,  $\alpha = \tilde{U}^-/\tilde{U}^+$ , and  $\tilde{U}^\pm$  the amplitudes of the two wave components.

For  $\alpha = 0$ , Eq. (1) describes a constant strain rotating with frequency  $\omega/2$  around the  $x_3$ -axis, which, in the gravity wave example, is associated with particle orbits that are perfectly circular [11]. Transforming to the rotating reference frame leads to the new expression for the strain field

$$\mathbf{E} = e \begin{pmatrix} \alpha \sin 2\omega t, & 1 + \alpha \cos 2\omega t \\ 1 + \alpha \cos 2\omega t, & -\alpha \sin 2\omega t \end{pmatrix} \quad (3)$$

(the initial phase of the rotation has been chosen to produce, at  $t = 0$ , a strain field with expanding direction at  $\pi/4$  with respect to the new  $x_1$  axis; see Appendix A). In the rotating reference frame, an additional vorticity field is produced:

$$\mathbf{\Omega} = \frac{\omega}{2} \begin{pmatrix} 0 & 1 \\ -1 & 0 \end{pmatrix}. \quad (4)$$

For  $\alpha \neq 0$ , this is a time-dependent planar flow, of the kind discussed in [3], which is known to produce aperiodic behaviors in the particle orientation dynamics.

The motion of a revolution ellipsoid, with symmetry axis identified by the versor  $\mathbf{p}$ , in the presence of the strain and vorticity fields  $\mathbf{E}$  and  $\mathbf{\Omega}$ , is described by the Jeffery's equations [1]:

$$\dot{\mathbf{p}} = \mathbf{\Omega} \cdot \mathbf{p} + G[\mathbf{E} \cdot \mathbf{p} - (\mathbf{p} \cdot \mathbf{E} \cdot \mathbf{p})\mathbf{p}]. \quad (5)$$

The parameter  $G$  gives the ellipsoid eccentricity, defined in terms of the particle aspect ratio  $r = a/b$ , where  $a$

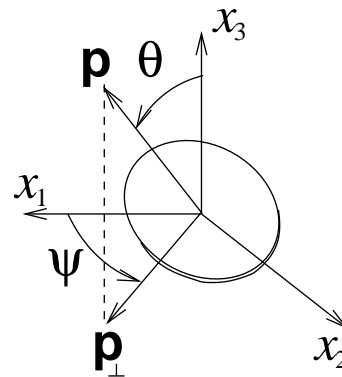


FIG. 1: The coordinate system. The axes  $x_i$  are in the rotating reference frame.

and  $b$  are respectively along and perpendicular to the symmetry axis, by means of the relation

$$G = \frac{r^2 - 1}{r^2 + 1}.$$

Introducing polar coordinates (see Fig. 1) and normalizing time and vorticity by the strain strength  $e$ :  $\omega \rightarrow \omega/(-2Ge)$  and  $t \rightarrow -Get$ , the Jeffery's equation (5), using Eqs. (3) and (4), will take the form:

$$\begin{cases} \dot{\psi} = -\omega + \beta(\psi, t), \\ \dot{c} = -\frac{1}{2}\beta'(\psi, t)c, \end{cases} \quad (6)$$

with  $c = \tan \theta$ , dot and prime indicating respectively  $d/dt$  and  $\partial/\partial\psi$ , and:

$$\begin{cases} \beta(\psi, t) = -\cos 2\psi - \alpha \cos(4\omega t + 2\psi), \\ \beta'(\psi, t) = 2[\sin 2\psi + \alpha \sin(4\omega t + 2\psi)] \end{cases} \quad (7)$$

(more details in Appendix A).

Following [3], the orbits can be classified studying the Poincare map  $P_n(\bar{\psi}) = \text{mod}(\psi(nT | \bar{\psi}), \pi)$ , with  $T = \frac{\pi}{2\omega}$  the period of  $\beta$ , where  $\psi(t|\bar{\psi})$  obeys the first of Eq. (6) with  $\psi(0|\bar{\psi}) = \bar{\psi}$ . This eliminates the explicit time dependence from the dynamics, and will allow to isolate the slow, noise produced deviation between orbits, from the fast motion along them (see next sections).

Some properties of the Poincare map can be obtained from inspection of Eqs. (6-7). In particular, it is possible to see, from  $\beta(\psi, t) = \beta(-\psi, -t)$  and the form of Eq. (6), that the following relation holds:

$$P_{-n}(-\bar{\psi}) = -P_n(\bar{\psi}), \quad (8)$$

and therefore the Poincare map is symmetric under the double reflection  $\{\psi, P_n\} \rightarrow \{\pi - \psi, \pi - P_n\}$  (see Fig. 2). This has the consequence that fixed points, when present, would come in pairs located symmetrically around  $\psi = \pi/2$  (see Fig. 3a).

A fixed point in the Poincare map will be associated with a periodic  $\psi$  and correspond to coherent orientation

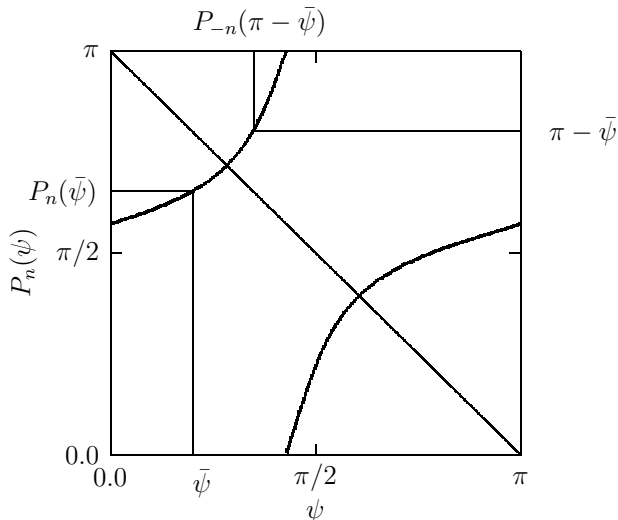


FIG. 2: Symmetry of the Poincaré map for the dynamics of Eqs. (6,7). Values of the parameters:  $\omega = 1.4$ ,  $\alpha \simeq 0.37$ ,  $n = 1$ ;  $G < 0$  (oblate ellipsoid). From Eq. (8), one has that  $P_{-n}(\pi - \psi) = \pi - P_n(\psi)$  and therefore the plot is symmetric under reflection across the diagonal line  $P_n = \pi - \psi$ .

of the particles. This regime is clearly produced by the aligning effect of strain on the particle dynamics, which becomes dominant in the small  $\omega$  range. In the present case, Eqs. (6-7) appear to lead at most to a pair of fixed points, of which the stable one is located at  $\psi > \pi/2$  (see Fig. 3a). The stable fixed point tends to  $\psi = 3\pi/4$  at  $\omega = 0$ , corresponding to alignment of the long ellipsoid axis with the strain expanding direction.

A transition to a coherent orientation regime is predicted in the case of a deep gravity wave [12] at the crossover frequency  $\omega_c = 1$  (no superposition of regressive and progressive components). Now, at  $\omega_c \simeq 1$ , the small wave amplitude approximation, leading to Eqs. (6-7) ceases to be valid (back to dimensional units, one would have for the particle displacement  $\Delta x \sim \tilde{U}/\omega_c \sim k^{-1}$ ). Nonetheless, the linearized theory provides a qualitatively correct picture, as a transition to a coherent orientation regime is observed experimentally in wave tanks, although with a larger transition frequency  $\omega_c \simeq 1.43$  [9]. The presence of a coherent orientation regime appears to be preserved for  $\alpha \neq 0$  with a crossover frequency  $\omega_c$  slowly decreasing as  $\alpha \rightarrow 1$  (at  $\alpha \simeq 0.82$ , one has still  $\omega_c \simeq 0.7$ ). The decrease in the crossover frequency can be explained in terms of the destabilization of the fixed particle orientation in the rotating frame, by the oscillating strain component of Eq. (3).

The alternative regime of random particle orientation, is associated with  $|\psi(nT)|$  increasing monotonously with  $n$ , with  $P_n(\psi)$  generally aperiodic. In this case, from continuity of  $\psi(t|\psi)$ ,  $P_n(\psi)$  will be topologically equivalent to an irrational rotation, and the sequence  $P_n(\psi)$  originating from a single  $\psi$  will fill densely the interval  $[0, \pi]$ .

An ergodic property is then satisfied, i.e. it is possible to calculate averages over  $\psi$  as time averages. Furthermore, from Poincaré recurrence, the  $P_n(\bar{\psi})$  sequence will come arbitrarily close to the initial condition for some  $n$ .

An important property is the following: if the orbit starting from a certain  $\bar{\psi}$  is approximately closed at  $t = nT$ , as shown in Fig. 3b, the same will occur with the orbits starting from any other initial condition. In fact, if  $P_n(\bar{\psi}) - \bar{\psi}$  is small, the same will be true also for  $P_n(P_m(\bar{\psi})) - P_m(\bar{\psi})$  with  $m$  arbitrary. This is consequence of the dynamics of  $\psi$  being not chaotic (i.e. neighbouring trajectories do not separate asymptotically). Hence, exploiting the fact that, from ergodicity,  $P_m(\psi)$  fills densely the whole interval  $[0, \pi]$ ,  $P_n(\psi) - \psi$  will be small for  $\psi$  generic.

Turning to the polar angle, if the orbit in  $\psi$  is approximately closed at  $nT$ , also  $c(nT|\bar{c}, \bar{\psi})$  will come arbitrarily close to the initial condition  $c(0|\bar{c}, \bar{\psi}) = \bar{c}$ . Hence, to identify approximately closed orbits, it is sufficient to look for recurrence of the Poincaré map  $P_n(\bar{\psi})$ . To see why this property holds, the two of Eq. (6) can be integrated to give:

$$\ln \frac{c(nT|\bar{c}, \bar{\psi})}{\bar{c}} = -\frac{1}{2} \ln \frac{\partial P_n(\bar{\psi})}{\partial \bar{\psi}},$$

and the condition  $c(nT|\bar{c}, \bar{\psi}) \simeq \bar{c}$  will be satisfied provided  $\partial P_n/\partial \bar{\psi} \simeq 1$ . In the present case, the condition  $\partial P_n/\partial \bar{\psi} \simeq 1$  is satisfied provided  $P_n(\bar{\psi}) \simeq \bar{\psi}$ , i.e. if the orbit is approximately closed. The contrary would require  $\partial P_n/\partial \bar{\psi}$  to oscillate in  $\bar{\psi}$  around  $\partial P_n/\partial \bar{\psi} = 1$ . However, if  $|P_n(\bar{\psi}) - \bar{\psi}| < \epsilon$  for some small  $\epsilon$ , the difference  $\partial P_n/\partial \bar{\psi} - 1$  could remain of  $O(1)$  in intervals at most of length  $O(\epsilon)$ , in which one would have in consequence  $\partial^2 P_n/\partial \bar{\psi}^2 = O(\epsilon^{-1})$ . But this is prevented from smoothness of the trajectories and of the functions  $\beta$  and  $\beta'$ .

### III. THE EFFECT OF NOISE

#### A. Coherent orientation regime

Noise produces qualitatively different effects in the coherent and in the random orientation regimes. In the coherent orientation regime, the main effect is smearing the transition to the random orientation regime. It is easier to describe what happens at the transition for  $\alpha = 0$ , where analytical expressions for  $\psi(t)$  and  $c(t)$  are available. When the crossover frequency  $\omega_c = 1$  is approached from above, i.e. from the random orientation regime, the rotation period for  $\psi$ :  $T_r$ , in the absence of noise, will tend to infinity like  $(\omega^2 - 1)^{-\frac{1}{2}}$  [12]. For  $\omega < 1$ , the particle is stuck at the stable fixed point  $\bar{\psi} = (\cos^{-1} \omega + \pi)/2$  and the period is by definition infinite. It turns out, that adding a small noise eliminates divergence of  $T_r$  for  $\omega \rightarrow \omega_c$ , as noise allows the particle to escape from the fixed point.

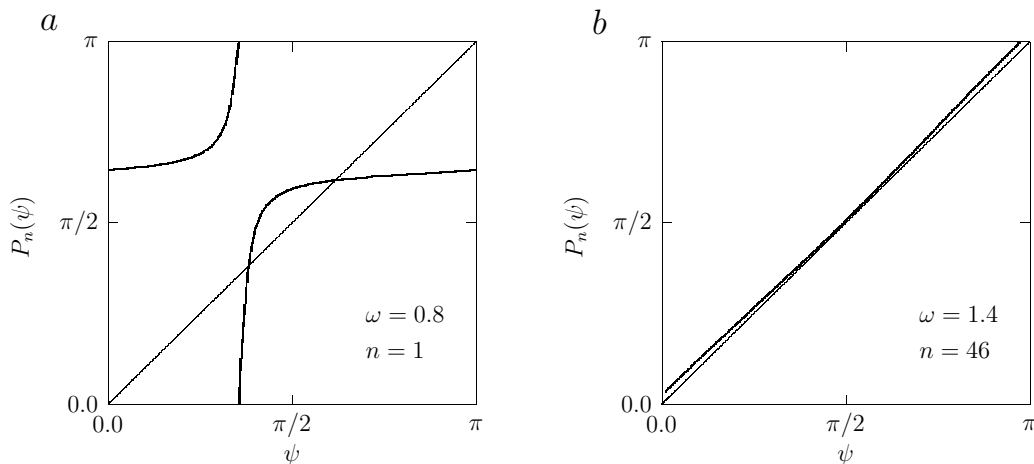


FIG. 3: Poincaré map for the coherent orientation (a) and the random orientation regime (b) of an oblate ellipsoid in a shallow water wave with  $\alpha \simeq 0.37$ . Notice in case (a) the stable fixed point at  $\psi > \pi/2$  and the unstable one at  $\psi < \pi/2$ . With prolate ellipsoids, the fixed points would have been exchanged. The value of  $n$  in the random orientation case (b) has been chosen to lead to approximately closed orbits. Notice that  $\psi = \pi/2$  remains the best approximation to a fixed point (i.e. a closed orbit of period  $nT$ ).

The time of escape from the fixed point can be expressed in terms of the inverse of the probability for  $\psi$  to reach the border of the basin of attraction for  $\bar{\psi}$ , which is  $\psi = \pi/2$ ; in other words:  $T_r^{-1} \sim P(\psi < \pi/2)$ . The probability  $P(\psi < \pi/2)$  could be roughly estimated, approximating the dynamics of  $\psi$  by the one of the Langevin equation obtained through linearization around  $\bar{\psi}$ , in the presence of noise, of the first of Eq. (6):

$$d\psi = 2(\psi - \bar{\psi}) \sin 2\bar{\psi} dt + D^{\frac{1}{2}} dW.$$

Here  $dW$  is the Brownian noise increment (Wiener process [13]):  $\langle dW \rangle = 0$ ,  $\langle dW^2 \rangle = dt$ , and  $D$  is supposed small. This Langevin equation leads to the PDF (probability density function) for  $\psi$  [13]:

$$\rho(\psi) = \text{const.} \exp\left(-\frac{2|\sin 2\bar{\psi}|}{D}(\psi - \bar{\psi})^2\right).$$

For small values of  $D$ ,  $P(\psi < \pi/2) \sim \rho(\pi/2)$  and therefore:

$$T_r \sim \exp\left(\frac{2|\sin 2\bar{\psi}|}{D}(\bar{\psi} - \pi/2)^2\right).$$

Thus, the rotation period is exponentially long in the inverse noise amplitude and the effect of Brownian rotations on the orientation distribution, which is governed by the stable fixed point of  $P_n(\psi)$ , will vanish in the zero noise limit.

## B. Random orientation regime

In the random orientation regime, the role of noise in determining an equilibrium orientation distribution is

fundamental. If Brownian rotations were strictly zero, the evolution of the PDF  $\rho(\psi, c; t)$  would be given by propagation along the unperturbed trajectories described by Eq. (6), which, from now on, will be identified by subscript zero:

$$\rho(\psi_0(t|\bar{\psi}), c_0(t|\bar{c}, \bar{\psi}); t) = \rho(\bar{\psi}, \bar{c}; 0)J(\bar{\psi}, \bar{c}), \quad (9)$$

where  $J(\bar{\psi}, \bar{c}) = |\det[(d\psi_0, dc_0)/(d\bar{\psi}, d\bar{c})]|^{-1}$  is the Jacobian of the transformation  $\{\psi, c\} \rightarrow \{\psi^0, c^0\}$ . This PDF is itself recurrent at the recurrence times  $t_i = n_i T$ ,  $i = 1, 2, \dots$ , for which  $P_{n_i}^0(\bar{\psi}) \simeq \bar{\psi}$ , and therefore also  $c_0(t_i|\bar{c}, \bar{\psi}) \simeq \bar{c}$  (see the end of last section). Hence, memory of any initial PDF  $\rho(c, \psi; 0)$  would be preserved at arbitrary large  $t_i$ :  $\rho(c, \psi; t_i) \simeq \rho(c, \psi; 0)$  and no relaxation to equilibrium would be possible.

Adding noise allows to reach statistical equilibrium in a time of the order of the inverse of the noise amplitude. Restricting to the discrete times  $nT$ , to make the process stationary, the equilibrium PDF for  $\psi$  is obtained from ergodicity and is the unique stationary PDF  $\rho_E(\psi) = \text{const.} |\omega + \beta(\psi, 0)|^{-1}$ . The statistics of  $c$ , can then be described in terms of the conditional PDF  $\rho(c|\psi) = \rho_E(\psi, c)/\rho_E(\psi)$ , where  $\rho_E(\psi, c)$  is the equilibrium joint PDF at the instants  $t = nT$ . Notice that, from ergodicity of  $\psi$ , it is sufficient to prescribe the form of  $\rho(\bar{c}|\bar{\psi})$  at a single position  $\bar{\psi}$ . In fact, to obtain  $\rho(c|\psi)$  at  $\psi \neq \bar{\psi}$ , to lowest order in the noise, it is sufficient to propagate Eq. (9) to  $t = nT$  and exploit the fact that  $P_n^0(\bar{\psi}) = \text{mod}(\psi_0(nT|\bar{\psi}), \pi)$  is dense in  $[0, \pi]$ .

The first step to obtain a kinetic equation for  $\rho(\bar{c}|\bar{\psi})$ , is to calculate the noise produced trajectory separation  $\{c(t|\bar{c}, \bar{\psi}) - c_0(t|\bar{c}, \bar{\psi}), \psi(t|\bar{\psi}) - \psi_0(t|\bar{\psi})\}$  at the recurrence times  $t = t_i$ , where, choosing appropriately  $t_i$ , the differences  $c_0(t_i|\bar{c}, \bar{\psi}) - \bar{c}$  and  $P_{n_i}^0(\bar{\psi}) - \bar{\psi}$  can be made small at

pleasure. However, since the conditioning in  $\rho(\bar{c}|\bar{\psi})$  is at  $\bar{\psi}$  and not at  $\psi(t|\bar{\psi})$ , it is then necessary to correct the first step and calculate the deviation  $c(t|\bar{c}, \bar{\psi}) - c_0(t|\bar{c}, \bar{\psi})$  at the time  $\hat{t}_i$  (equal to  $t_i$  only in the zero noise limit), at which  $\text{mod}(\psi(\hat{t}_i|\bar{\psi}), \pi)$  and  $\bar{\psi}$  are strictly equal. This means considering, instead of a Poincare map synchronized with the period of  $\beta$ , the one synchronized with the rotation period in  $\psi$ , i.e. with the crossing of  $\bar{\psi}$  by  $\psi$ .

Accounting for the effect of Brownian rotations, the Jeffery's equations will read (see Appendix B):

$$\begin{cases} d\psi = [-\omega + \beta(\psi, t)]dt + D^{1/2}g^{1/2}(c)dW_\psi, \\ dc = [-\frac{1}{2}\beta'(c, t)c + Df(c)]dt + D^{1/2}h^{1/2}(c)dW_c, \end{cases} \quad (10)$$

where  $D$  has the meaning of a diffusion constant (in the present dimensionless units,  $D^{-1} = Pe$ ),  $dW_k$ , with  $k = \psi, c$ , are the Brownian increments:

$$\langle dW_k \rangle = 0, \quad \langle dW_k dW_j \rangle = \delta_{kj} dt, \quad (11)$$

and the functions  $f$ ,  $g$  and  $h$  are given by (see again Appendix B):

$$\begin{aligned} f(c) &= \frac{1}{c}(1+c^2)\left(\frac{1}{2}+c^2\right), \\ g(c) &= \frac{1}{c^2} + 1 \quad \text{and} \quad h(c) = (1+c^2)^2. \end{aligned} \quad (12)$$

The unperturbed orbits, as already mentioned, indicated by  $\{\psi_0, c_0\}$ , obey Eq. (6):

$$\begin{cases} \dot{\psi}_0 = -\omega + \beta_0, \\ \dot{c}_0 = -\frac{1}{2}\beta'_0 c_0, \end{cases} \quad (13)$$

with  $\beta_0 = \beta(\psi_0, t)$  and similar definition for  $\beta'_0$ . For small noise, the correction can be determined as an expansions in powers of  $D^{1/2}$ :  $\psi = \psi_0 + \psi_{1/2} + \psi_1 + \dots$  and similarly for  $c$ , with the initial condition  $\psi_k(0) = c_k(0) = 0$  for  $k > 0$ . The lowest order correction is obtained from linearization of Eq. (10) around  $\{\psi_0, c_0\}$ :

$$\begin{cases} d\psi_{1/2} = \beta'_0 \psi_{1/2} dt + D^{1/2}g_0^{1/2} dW_\psi, \\ dc_{1/2} = [2\beta_0 c_0 \psi_{1/2} - \frac{1}{2}\beta'_0 c_{1/2}]dt + D^{1/2}h_0^{1/2} dW_c. \end{cases} \quad (14)$$

From Eq. (11) and from linearity of Eq. (14)  $\langle \psi_{1/2} \rangle = \langle c_{1/2} \rangle = 0$ , but  $\psi_{1/2}$  and  $c_{1/2}$  are not zero. The covariance equations obtained from Eq. (14) are:

$$\begin{cases} \frac{d}{dt} \langle \psi_{1/2}^2 \rangle = 2\beta'_0 \langle \psi_{1/2}^2 \rangle + Dg_0, \\ \frac{d}{dt} \langle \psi_{1/2} c_{1/2} \rangle = \frac{1}{2}\beta'_0 \langle \psi_{1/2} c_{1/2} \rangle + 2\beta_0 c_0 \langle \psi_{1/2}^2 \rangle, \\ \frac{d}{dt} \langle c_{1/2}^2 \rangle = 4\beta_0 c_0 \langle \psi_{1/2} c_{1/2} \rangle - \beta'_0 \langle c_{1/2}^2 \rangle + Dh_0, \end{cases} \quad (15)$$

and lead to a diffusion contribution to the deviation. To obtain the drift contributions, it is necessary to consider the next order in the expansion of Eq. (10), and the result is:

$$\begin{cases} \frac{d}{dt} \langle \psi_1 \rangle = \beta'_0 \langle \psi_1 \rangle - 2\beta_0 \langle \psi_{1/2}^2 \rangle, \\ \frac{d}{dt} \langle c_1 \rangle = -\frac{1}{2}\beta'_0 \langle c_1 \rangle + 2\beta_0 c_0 \langle \psi_1 \rangle \\ \quad + 2\beta_0 \langle \psi_{1/2} c_{1/2} \rangle + \beta'_0 c_0 \langle \psi_{1/2}^2 \rangle + Df_0. \end{cases} \quad (16)$$

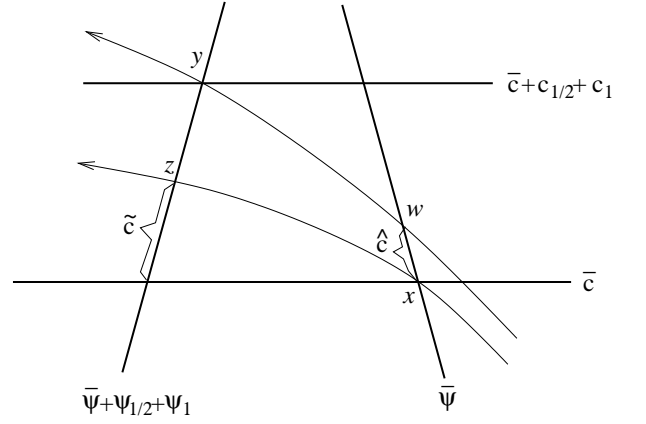


FIG. 4: Orbit behavior in the proximity of the recurrent point  $x = \{\bar{\psi}, \bar{c}\}$ ;  $x - z$  unperturbed orbit;  $w - y$  noisy orbit. The deviation between orbits is identified by  $\hat{c}$ .

The lowest order contributions to diffusion and drift are therefore both  $O(D)$ , as they should. Some simplifications of Eqs. (13), (15) and (16), taking care of the singularities of Eq. (12) at  $c = 0$ , are still possible and are illustrated in Appendix C.

Once the noisy trajectory  $\{\psi(t|\bar{\psi}), c(t|\bar{c}, \bar{\psi})\}$  has been calculated up to the recurrence time  $t_i$ , it is necessary to follow it back to the time  $\hat{t}_i$  at which  $\text{mod}(\psi(\hat{t}_i|\bar{\psi}), \pi) = \bar{\psi}$  and calculate the difference

$$\hat{c} = c(\hat{t}_i|\bar{c}, \bar{\psi}) - c_0(t_i|\bar{c}, \bar{\psi}) \simeq c(\hat{t}_i|\bar{c}, \bar{\psi}) - \bar{c}.$$

This operation is equivalent to the procedure, implicit in [8], of subtracting from the deviation  $\{\psi(t_i|\bar{\psi}) - \psi_0(t_i|\bar{\psi}), c(t_i|\bar{c}, \bar{\psi}) - c_0(t_i|\bar{c}, \bar{\psi})\} \simeq \{\psi_{1/2} + \psi_1, c_{1/2} + c_1\}$ , the component along the unperturbed Jeffery's orbit, and keeping only the part associated with percolation between the orbits. The necessary operations are illustrated in Fig. 4, and it is assumed that the orbits can be parameterized locally with  $\psi \equiv \psi_0(t|\bar{\psi})$  (this is possible if  $\bar{\psi}$  is chosen away from turning points). The first step is to calculate the difference in  $c$  between noisy and unperturbed orbits, at the azimuthal angle  $\psi = \psi(t_i|\bar{\psi})$  where  $\text{mod}(\psi(t_i|\bar{\psi}), \pi) \simeq \bar{\psi} + \psi_{1/2} + \psi_1$ , corresponding to the points  $y$  and  $z$  in Fig. 4. To  $O(D)$ , the value of  $c$  at  $z$  is

$$\bar{c} + \tilde{c} = \bar{c} + c_\psi(\psi_{1/2} + \psi_1) + \frac{1}{2}c_{\psi\psi}\psi_{1/2}^2, \quad (17)$$

where  $c_\psi$  and  $c_{\psi\psi}$  give the rise in  $c$  along the unperturbed trajectory:

$$c_\psi = \frac{dc_0}{d\psi} \quad \text{and} \quad c_{\psi\psi} = \frac{d^2c_0}{d\psi^2}, \quad (18)$$

with  $d/d\psi$  the derivative along the unperturbed orbit:

$$\frac{d}{d\psi} = \frac{1}{\dot{\psi}_0} \left[ \frac{\partial}{\partial t} + \dot{\psi}_0 \frac{\partial}{\partial \psi} + \dot{c}_0 \frac{\partial}{\partial c} \right], \quad (19)$$

which is calculated at  $\psi = \bar{\psi}$ . Combining Eqs. (18-19) with Eq. (13):

$$\begin{cases} c_\psi = \frac{\beta' c_0}{2(\omega - \beta_0)}, \\ c_{\psi\psi} = -\frac{\beta_0 \beta_0' c_0}{(\omega - \beta_0)^3} + \frac{(\beta_0'^2 - \beta_0') c_0}{(\omega - \beta_0)^2} - \frac{2\beta_0 c_0}{\omega - \beta_0}, \end{cases} \quad (20)$$

where  $\hat{\beta} = \partial_t \beta$  and similar for  $\hat{\beta}'$ . To obtain  $\hat{c}$ , it is necessary to correct the difference in  $c$  between  $y$  and  $z$ , i.e.  $c_{1/2} + c_1 - \tilde{c}$ , for the contribution from the deviation between unperturbed orbits, which, in the present case, is  $(c_{1/2} + c_1 - \tilde{c})(\psi_{1/2} + \psi_1)c_{\psi c}$ , where

$$c_{\psi c} = \partial c_\psi / \partial c = c_0^{-1} c_\psi. \quad (21)$$

Working again to  $O(D)$ :

$$\hat{c} = c_{1/2} + c_1 - \tilde{c} - \psi_{1/2} c_{\psi c} (c_{1/2} - \tilde{c}), \quad (22)$$

corresponding to a time along the trajectory:

$$\hat{t}_i = t_i + [\omega + \beta(\bar{\psi}, 0)]^{-1} \psi_{1/2} + O(D). \quad (23)$$

Using the relation  $\langle \psi_{1/2} c_{1/2} \rangle = -c_0 \langle \psi_1 \rangle$  (see Appendix C), together with Eqs. (17) and (22), the following result for the diffusion and drift across Jeffery's orbits is obtained, to  $O(D)$ :

$$\begin{cases} \langle \hat{c}^2 \rangle = \langle c_{1/2}^2 \rangle + c_\psi^2 \langle \psi_{1/2}^2 \rangle - 2c_\psi \langle \psi_{1/2} c_{1/2} \rangle, \\ \langle \hat{c} \rangle = \langle c_1 \rangle + (c_\psi c_{\psi c} - \frac{1}{2} c_{\psi\psi}) \langle \psi_{1/2}^2 \rangle, \end{cases} \quad (24)$$

and, combining with Eqs. (20) and (21), the noise induced deviation between Jeffery orbits is fully determined.

#### IV. DETERMINATION OF THE ORIENTATION DISTRIBUTION

The quantities  $\langle \hat{c}^2 \rangle$  and  $\langle \hat{c} \rangle$  allow to determine the noise contribution to orbit deviation, at the corrected recurrence times  $\hat{t}_i$ , at which  $\text{mod}(\psi(\hat{t}_i|\bar{\psi}), \pi) = \bar{\psi}$ . Both quantities  $\langle \hat{c}^2 \rangle$  and  $\langle \hat{c} \rangle$  are obtained from integrals along the orbits and it is expected that an averaging process takes place, with  $\langle \hat{c}^2 \rangle / t_i$  and  $\langle \hat{c} \rangle / t_i$  tending to finite limits as  $t_i \rightarrow \infty$ . Integrating numerically Eqs. (13) and (15-16) [or, more simply, Eq. (C2)], with the initial condition  $\{\psi_0(0|\bar{\psi}), c_0(0|\bar{c}, \bar{\psi})\} = \{\bar{\psi}, \bar{c}\} = \{0, 0\}$  and then substituting, with Eqs. (20-21), into (24), leads to the result in Fig. 5. Self-averaging of  $\langle \hat{c}^2 \rangle / t_i$  takes place also for relatively large values of the tolerance  $\epsilon$ , which identifies recurrence, and therefore the sequence  $t_i = t_i(\epsilon)$   $i = 1, 2, \dots$ , through the condition  $|P_n^0(\bar{\psi}) - \bar{\psi}| < \epsilon$ . It is thus possible to introduce effective drift and diffusion coefficients  $\bar{a}$  and  $\bar{D}$ :

$$\bar{a}(\bar{c}, \bar{\psi}) = \lim_{i \rightarrow \infty} t_i^{-1} \langle \hat{c} \rangle, \quad \bar{D}(\bar{c}, \bar{\psi}) = \lim_{i \rightarrow \infty} t_i^{-1} \langle \hat{c}^2 \rangle, \quad (25)$$

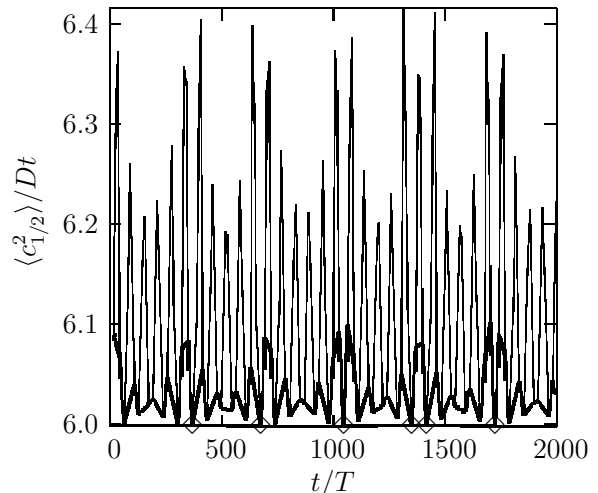


FIG. 5: Determination of the normalized diffusivity  $\langle c_{1/2}^2 \rangle / Dt$  for different values of the tolerance  $\epsilon$  entering the recurrence condition  $|P_n(\bar{\psi}) - \bar{\psi}| < \epsilon$  with  $\{\bar{\psi}, \bar{c}\} = \{0, 0\}$ . Values of the parameters  $\omega = 1.4$ ,  $\alpha \simeq 0.37$ . Thin line  $\epsilon = 0.4$ ; heavy line  $\epsilon = 0.1$ ; diamonds  $\epsilon = 0.01$  (the diamonds identify the actual position of the recurrence times).

which will describe the dynamics of the Poincare map  $\bar{c}(\hat{t}_i) \equiv c(\hat{t}_i|\bar{c}(0), \bar{\psi})$ :

$$\bar{c}(\hat{t}_i) - \bar{c}(0) = \bar{a} \hat{t}_i + \bar{D}^{1/2} [W(\hat{t}_i) - W(0)]. \quad (26)$$

This is a discrete Langevin equation, in which  $W(t)$  is again the Wiener process, with  $\langle [W(t) - W(0)]^2 \rangle = t$ . In the small  $D$  limit, the recurrence times  $t_i$  can be treated as continuous on the scale of the relaxation to equilibrium. It is then possible to obtain a Fokker-Planck equation for the evolution of the PDF for  $\bar{c}(t)$ , which, by construction, is nothing else than  $\rho(\bar{c}|\bar{\psi})$ . Now, from Eq. (23):

$$\rho(\bar{c}|\bar{\psi}; \hat{t}_i) - \rho(\bar{c}|\bar{\psi}; 0) = [1 + O(D^{1/2})] t_i \partial_t \rho(\bar{c}|\bar{\psi}; t)|_{t=0},$$

and, to lowest order in  $D$ , it is possible to disregard the difference between  $\hat{t}_i$  and  $t_i$  in  $\rho$ ; this is equivalent to substitute  $\bar{c}(t_i) - \bar{c}(0)$  into the left hand side of Eq. (26). Taking the continuous limit, leads to the Langevin equation  $d\bar{c} = \bar{a} dt + \bar{D}^{1/2} dW$ , which is associated with the Fokker-Planck equation [13]:

$$\partial_{\bar{t}} \rho + \partial_{\bar{c}} (\bar{a} \rho) = \frac{1}{2} \partial_{\bar{c}}^2 (\bar{D} \rho), \quad (27)$$

and the notation  $\bar{t}$ , indicating a slow time scale, is a reminder that Eq. (27) is meaningful only at timescales long with respect to  $t_i - t_{i-1}$ . Slow variation of the flow parameters entering Eq. (10) would lead to dependence of the coefficients in Eq. (27) on the slow time  $\bar{t}$ . As in [8], the fact that both  $\bar{a}$  and  $\bar{D}$  depend linearly in  $D$

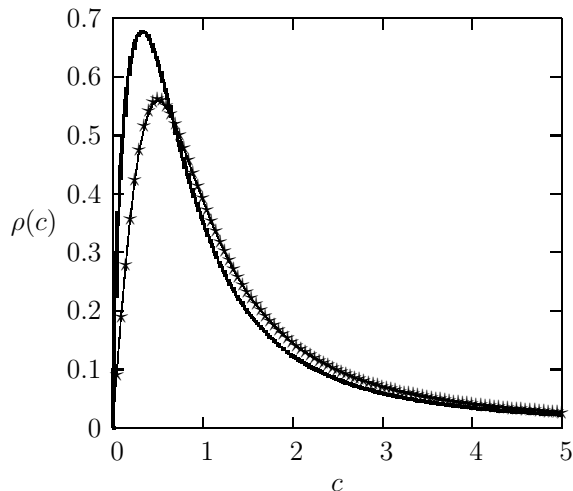


FIG. 6: Comparison of the PDF  $\rho(\bar{c}|\bar{\psi})$  calculated using for  $\bar{a}$  and  $\bar{D}$  different values of  $t_i$  [see Eq. (25)]. Values of the parameters:  $\omega = 1.4$ ,  $\alpha = 0$ ,  $\bar{\psi} = 0$ . Heavy line:  $t_i = 3T$   $\epsilon = 0.4$ ; stars:  $t_i = 20T$ ,  $\epsilon = 0.1$ ; thin line: Leal & Hinch theory [8].

implies that the equilibrium PDF is independent of the noise amplitude.

As statistical equilibrium will be achieved on the time scale  $D^{-1}$ , in order for the approach to be meaningful, it is necessary that the  $t_i$  used to define  $\bar{a}$  and  $\bar{D}$  satisfy  $Dt_i \ll 1$ . Actually, excellent convergence is obtained already for  $t_i$  rather small; in the case of Fig. 6, at  $t_i = 20T$ , corresponding to  $\epsilon = 0.1$ . Notice that the case considered in Fig. 6, which is identical to the deep water wave regime considered in [12], can be mapped to a constant simple shear by a redefinition of the eccentricity  $G$ . [In this case, the aperiodicity of  $P_n^0(\bar{\psi})$  originates not from the dynamics, but from the sampling time  $T$  and the rotation period  $T_r = (\omega^2 - 1)^{-\frac{1}{2}}$  being incommensurate]. The PDF  $\rho(\bar{c}|\bar{\psi})$  can then be compared with the analytical result from the theory of Leal and Hinch [the function  $f(C)$  in Eq.(17) of their paper] [8]. As can be seen from Fig. 6, the two approaches give indistinguishable results already for  $t_i = 20T$ ,  $\epsilon = 0.1$ . Similar convergence to the limit result is observed for  $\alpha > 0$ , when comparison with the theory of Leal and Hinch is not possible.

Knowledge of the PDF  $\rho(\bar{c}|\bar{\psi})$  allows determination of the effective viscosity of a dilute disk suspension in the oscillating strain field of Eq. (1). The viscous stress for a suspension of axisymmetric ellipsoids reads [8, 14], indicating with  $\mu$  and  $\Phi$ , respectively, the solvent viscosity and the suspended phase volume fraction:

$$\begin{aligned} \boldsymbol{\sigma} = & 2\mu\mathbf{E} + 2\mu\Phi\{2A\langle\mathbf{p}\mathbf{p}\mathbf{p}\mathbf{p}\rangle : \mathbf{E} \\ & + 2B[\langle\mathbf{p}\mathbf{p}\rangle \cdot \mathbf{E} + \mathbf{E} \cdot \langle\mathbf{p}\mathbf{p}\rangle] + C\mathbf{E}\}, \end{aligned} \quad (28)$$

where, in the present time dependent situation, the averages are intended over orientation and time. The coef-

ficients  $A - C$  depend on the particle geometry [12]:

$$\begin{aligned} A = & \frac{5}{3\pi r} + \frac{104}{9\pi^2} - 1, \quad B = -\frac{4}{3\pi r} - \frac{64}{9\pi^2} + \frac{1}{2} \\ & \text{and } C = \frac{8}{3\pi r} + \frac{128}{9\pi^2}, \end{aligned}$$

with  $r$  the particle aspect ratio, supposed small. These expressions correct to  $O(1)$ , similar ones derived in [8]. From the stress  $\boldsymbol{\sigma}$ , the effective viscosity  $\bar{\mu}$  can be calculated in terms of the viscous dissipation in the suspension:

$$\bar{\mu} = \frac{1}{2} \frac{\boldsymbol{\sigma} : \mathbf{E}}{\mathbf{E} : \mathbf{E}} := (1 + K\Phi)\mu, \quad (29)$$

where  $K$  is called the reduced viscosity. Expressing the versor  $\mathbf{p}$  in function of the angles  $\psi$  and  $\theta$ , and using Eqs. (28) and (29):

$$K = A\langle\sin^4\theta\sin^22\psi\rangle + 2B\langle\sin^2\theta\rangle + C. \quad (30)$$

As in [8], the average over orientation is split into parts along and transverse to the orbit. In the present situation, however, evaluation of the average along the orbit is slightly more delicate than in the time-independent case. At a generic time  $t$  the average of a function  $f(\psi, c)$  will be:

$$\langle f \rangle(t) = \frac{1}{n} \sum_{i=1}^n \int d\bar{c} \rho(\bar{c}|\bar{\psi}) f(\psi(t+iT|\bar{\psi}), c(t+iT|\bar{c}, \bar{\psi})),$$

where, from ergodicity, memory of the initial condition  $\bar{\psi}$  is lost for  $n \rightarrow \infty$ . Carrying on the average over one period, which, in the case of a wave, from Eq. (2), is equivalent also to a space average, leads to the average along an orbit:

$$\langle f \rangle = \frac{1}{nT} \int d\bar{c} \rho(\bar{c}|\bar{\psi}) \int_0^{nT} dt f(\psi(t|\bar{\psi}), c(t|\bar{c}, \bar{\psi})). \quad (31)$$

Evaluating Eq. (30) with Eq. (31) leads to the values of the reduced viscosity shown in Fig. 7. The calculation has been carried on, using as recurrence point,  $\bar{\psi} = 0$ ; the value of the particle aspect ratio has been chosen consistent with frazil ice measurements [9]. The same qualitative regime observed for  $\alpha = 0$  is reproduced here, namely, a dip in the reduced viscosity at the crossover from the coherent rotation regime to the random orientation one [12].

In the case of gravity waves, the coherent regime would always be associated with high amplitude waves, corresponding to small values of the normalized frequency  $\omega$ . The reduced viscosity has been calculated in this range from Eq. (30), fixing  $\theta = \pi/2$  and integrating the equation for  $\psi$ , in the absence of noise, with initial condition at the fixed point.

## V. CONCLUSIONS

The numerical evaluation of the rheological properties of a suspension of particles that are weakly Brownian is

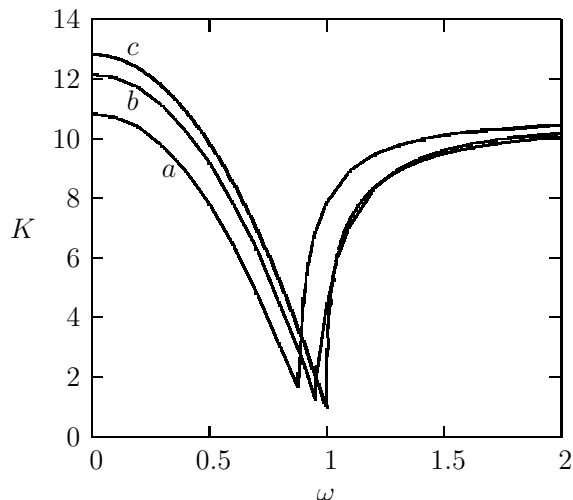


FIG. 7: Reduced viscosity, averaged over a period, for a suspension of disk-like particles with aspect ratio  $r = 0.045$ . In the three cases: (a)  $\alpha \simeq 0.61$ ; (b)  $\alpha \simeq 0.37$ ; (c)  $\alpha = 0$ .

faced with difficulties associated with the long integration times necessary to achieve statistical equilibrium. Analytical techniques for the calculation of the cumulative effect of the Brownian noise on the dynamics are therefore necessary. The technique presented in this paper can be seen as a multiple time scale analysis [15] in which the stochastic dynamics is pushed to the slow scale, while the local strain and vorticity are treated as fast variables. For the periodic flows considered in this paper, the effective drift and diffusivity coefficients are obtained integrating the fast (and aperiodic) orientation dynamics up to the first recurrence time, at which the approximation of a closed orbit is considered good enough. Slow variations would be accounted for, sampling the almost closed trajectory segments in appropriate way along the particle orbit, and would lead to effective drift and diffusivity coefficients depending on the slow time. Once the effective drift and diffusivity were available, a Monte Carlo, for the determination of the rheological properties of a suspension, would be carried on at the slow time scale [this would be associated formally with integration of the Fokker-Planck equation (27)].

Application of these techniques to the dynamics of a thin disk suspension in gravity waves, suggest that qualitative behaviors in deep water, accounted for theoretically in [12] and observed experimentally in [9], should be preserved in the shallow water regime. In particular, a transition from a coherent rotation regime for large amplitude waves to a random orientation one, marked by a deep minimum in the medium effective viscosity, should continue to be present. Away from this regime, in the random orientation regime, the numerical values of the effective viscosity appear to be only weakly dependent on the water depth. This strengthens confidence in ex-

perimental data on the sea ice effective viscosity from wave tanks, in which the deep water condition is at the most only approximately satisfied, as a test case of what happens in the open sea [9, 10].

A natural extension of the techniques illustrated could be the treatment of higher numbers of degrees of freedom. An interesting example is the triaxial ellipsoid in a simple shear considered in [4]. In this case, the angle  $\theta$  would be replaced by the pair  $\{\theta, \phi\}$  with  $\phi$  the rotation around the axis  $\mathbf{p}$ . An analysis in the whole phase domain would require, however, consideration of the transition region from the regular orbits, in which diffusion is dominated by Brownian rotation, to the chaos dominated stochastic region.

### Acknowledgments

This research was carried on at the Dipartimento di Fisica dell'Università di Cagliari. The author wishes to thank Alberto Pompei for hospitality.

### APPENDIX A: ORIENTATION DYNAMICS IN ROTATING REFERENCE FRAME

The strain matrix in the laboratory frame, is provided by Eq. (1). Passing to the rotating frame:

$$\mathbf{R} \cdot \mathbf{E} \cdot \mathbf{R}^T = \begin{pmatrix} 1 + \alpha \cos 2\omega t, & -\alpha \sin 2\omega t \\ -\alpha \sin 2\omega t, & -1 - \alpha \cos 2\omega t \end{pmatrix},$$

where

$$\mathbf{R} = \begin{pmatrix} \cos \omega t/2, & \sin \omega t/2 \\ -\sin \omega t/2, & \cos \omega t/2 \end{pmatrix}$$

is the matrix for an angle  $-\omega t/2$  rotation. In term of components,  $u_i$  and  $v_i = R_{ij}u_j$  are the components of a vector in the laboratory and the rotating reference frame. In the rotating frame, the fluid is seen rotating like  $v_i$ :

$$\dot{v}_i = \Omega_{ij}v_j, \quad \Omega = \frac{\omega}{2} \begin{pmatrix} 0, & 1 \\ -1, & 0 \end{pmatrix},$$

and  $\Omega$  is the vorticity of the fluid measured in the rotating frame. One more rotation by  $\pi/4$  produces Eq. (3)

$$\begin{aligned} & \hat{\mathbf{R}} \begin{pmatrix} 1 + \alpha \cos 2\omega t, & -\alpha \sin 2\omega t \\ -\alpha \sin 2\omega t, & -1 - \alpha \cos 2\omega t \end{pmatrix} \hat{\mathbf{R}}^T \\ &= \begin{pmatrix} \alpha \sin 2\omega t, & 1 + \alpha \cos 2\omega t \\ 1 + \alpha \cos 2\omega t, & -\alpha \sin 2\omega t \end{pmatrix}, \end{aligned}$$

where

$$\hat{\mathbf{R}} = \frac{1}{\sqrt{2}} \begin{pmatrix} 1, & -1 \\ 1, & 1 \end{pmatrix}.$$



As the next step, pass to adimensional variables:

$$\hat{t} = -Get, \quad \hat{\omega} = -\frac{\omega}{2Ge}, \quad \hat{\mathbf{E}} = e^{-1}\mathbf{E}.$$

This choice guarantees that, in the case of oblate ellipsoids, the signs of the normalized times and frequency are preserved. Substituting into the Jeffery's equation (5) gives:

$$\frac{d\mathbf{p}}{d\hat{t}} = \hat{\omega} \begin{pmatrix} 0, & 1 \\ -1, & 0 \end{pmatrix} \mathbf{p} - [\hat{\mathbf{E}} \cdot \mathbf{p} - (\mathbf{p} \cdot \hat{\mathbf{E}} \cdot \mathbf{p})\mathbf{p}]. \quad (\text{A1})$$

Introducing polar coordinates  $\mathbf{p} = (\sin \theta \cos \psi, \sin \theta \sin \psi, \cos \theta)$  and using Eq. (3), leads to the expressions:

$$\mathbf{E} \cdot \mathbf{p} = \sin \theta \begin{pmatrix} \sin \psi + \alpha \sin(\psi + 4\hat{\omega}t) \\ \cos \psi + \alpha \cos(\psi + 4\hat{\omega}t) \end{pmatrix} \quad (\text{A2})$$

and

$$\mathbf{p} \cdot \mathbf{E} \cdot \mathbf{p} = \sin^2 \theta [\sin 2\psi + \alpha \sin(2\psi + 4\hat{\omega}t)]. \quad (\text{A3})$$

The Jeffery's equation can now be written in components. Starting from  $\theta$ , using Eqs. (A1-A3):

$$\dot{p}_3 = -\sin \theta \dot{\theta} = \cos \theta \sin^2 \theta [\sin 2\psi + \alpha \sin(2\psi + 4\hat{\omega}t)], \quad (\text{A4})$$

which leads to the second of Eqs. (6-7). Passing to the equation for  $\psi$ :

$$\begin{aligned} \dot{p}_2 &= \sin \theta \cos \psi \dot{\psi} + \cos \theta \sin \psi \dot{\theta} = -\hat{\omega} \sin \theta \cos \psi \\ &\quad - \sin \theta [\cos \psi + \alpha \cos(\psi + 4\hat{\omega}t)] + \sin^3 \theta [\sin 2\psi \\ &\quad \quad + \alpha \sin(2\psi + 4\hat{\omega}t)] \sin \psi, \end{aligned}$$

from which, using Eq. (A4):

$$\begin{aligned} \cos \psi \dot{\psi} &= -\hat{\omega} \cos \psi - \cos \psi (1 - 2 \sin^2 \psi) \\ &\quad + \alpha [\sin(2\psi + 4\hat{\omega}t) \sin \psi - \cos(\psi + 4\hat{\omega}t)], \end{aligned}$$

and, after little algebra:

$$\dot{\psi} = -\hat{\omega} - \cos 2\psi - \alpha \cos(2\psi + 4\hat{\omega}t),$$

which is the first of Eqs. (6-7).

## APPENDIX B: NOISE TERM DETERMINATION

The noise term to add in Eq. (6) can be obtained directly from the diffusion equation obeyed for zero flow by the orientation PDF in the variables  $\{\psi, c\}$ . Alternatively, one may consider the diffusion operator in the variables  $\{\psi, \theta\}$ :

$$\nabla^2 = \frac{1}{\sin^2 \theta} \frac{\partial^2}{\partial \psi^2} + \frac{1}{\sin \theta} \frac{\partial}{\partial \theta} \sin \theta \frac{\partial}{\partial \theta},$$

and determine the stochastic process leading to the Fokker-Planck equation  $\nabla^2 \rho(\psi, \theta) = 0$  [which has the

isotropic solution  $\rho(\psi, \theta) = \frac{1}{2\pi} \sin \theta$ ]. One finds the increments for  $\psi$  and  $\theta$  produced by Brownian rotation in the time interval  $dt$  [13]:

$$d\psi = |\sin \theta|^{-1} dW_\psi, \quad d\theta = \frac{1}{2} \cot \theta dt + dW_\theta,$$

where  $dW_k$ ,  $k = \psi, \theta$  are the Brownian increments

$$\langle dW_k \rangle = 0, \quad \langle dW_j dW_k \rangle = \delta_{jk} dt.$$

Changing then variables from  $\theta$  to  $c$  and using Itô's lemma, one finds:

$$\begin{aligned} dc &= d\theta \frac{dc}{d\theta} + \frac{1}{2} \langle dW_\theta^2 \rangle \frac{d^2 c}{d\theta^2} \\ &= \frac{1}{c} (1 + c^2) \left( \frac{1}{2} + c^2 \right) dt + (1 + c^2) dW_\theta, \end{aligned}$$

and, using the expression  $\sin \theta = c(1 + c^2)^{-1/2}$  in  $d\psi$ , Eq. (10) is finally obtained.

## APPENDIX C: ALTERNATIVE FORM OF THE PERTURBED ORBIT EQUATION

Equations (15-16) can be simplified, and the singularity in  $\theta = 0$  produced by the noise term in the first of Eq. (10) eliminated, by the change of variables:

$$\begin{aligned} y_1 &= c_0^2 \langle \psi_{1/2}^2 \rangle, & y_2 &= c_0 \langle \psi_{1/2} c_{1/2} \rangle, \\ y_3 &= \langle c_{1/2}^2 \rangle, & y_4 &= c_0 \langle c_1 \rangle, & y_5 &= c_0^2 \langle \psi_1 \rangle. \end{aligned}$$

In the new variables, Eqs. (15-16) take the form:

$$\begin{cases} \dot{y}_1 = \beta'_0 y_1 + D\tilde{g}, \\ \dot{y}_2 = 2\beta_0 y_1, \\ \dot{y}_3 = 4\beta_0 y_2 - \beta'_0 y_3 + D\tilde{h}, \\ \dot{y}_4 = -\beta'_0 y_4 + 2\beta_0 y_2 + \beta'_0 y_1 + 2\beta_0 y_5 + D\tilde{f}, \\ \dot{y}_5 = -2\beta_0 y_1, \end{cases} \quad (\text{C1})$$

where, from Eq. (12),  $\tilde{g} = 1 + c_0^2$ ,  $\tilde{h} = (1 + c_0^2)^2$  and  $\tilde{f} = (1 + c_0^2)(\frac{1}{2} + c_0^2)$ . Comparing the equations for  $y_2$  and  $y_5$ , one sees that, thanks to the initial condition  $y_k(0) = 0$ ,  $y_2 = -y_5$  and then  $\langle \psi_{1/2} c_{1/2} \rangle = -c_0 \langle \psi_1 \rangle$ ; thus the equation for  $\langle \psi_1 \rangle$  can be eliminated from (16). Equation (C1) can then be further simplified to:

$$\begin{cases} \dot{y}_1 = \beta'_0 y_1 + D\tilde{g}, \\ \dot{y}_2 = 2\beta_0 y_1, \\ \dot{y}_3 = 4\beta_0 y_2 - \beta'_0 y_3 + D\tilde{h}, \\ \dot{y}_4 = -\beta'_0 y_4 + \beta'_0 y_1 + D\tilde{f}. \end{cases} \quad (\text{C2})$$

- 
- [1] G.B. Jeffery, "The motion of ellipsoidal particles immersed in a viscous fluid," *Proc. Roy. Soc. A* **102**, 161 (1922)
- [2] G.I. Taylor, "The motion of ellipsoidal particles in a viscous fluid," *Proc. Roy. Soc. A* **103**, 58 (1923)
- [3] A.J. Szeri, W.J. Milliken and L.G. Leal, "Rigid particles suspended in time-dependent flows: irregular versus regular motion, disorder versus order," *J. Fluid Mech.* **237**, 33 (1992)
- [4] A.L. Yarin, O. Gottlieb and I.V. Roisman, "Chaotic rotation of triaxial ellipsoids in simple shear flows," *J. Fluid Mech.* **340**, 83 (1997)
- [5] J.M. Burgers, *Second Report on Viscosity and Plasticity* (North-Holland, Amsterdam, 1938) Chap. 3
- [6] A. Peterlin, "Über die Viskosität von verdünnten Lösungen und Suspensionen in Abhängigkeit von der Teilchenform," *Z. Physik* **111**, 232 (1938)
- [7] H.A. Scheraga, "Non-Newtonian viscosity of solutions of ellipsoidal particles," *J. Chem. Phys.* **23**, 1526 (1955)
- [8] L.G. Leal and E.J. Hinch, "The effect of weak Brownian rotations on particles in shear flows," *J. Fluid. Mech.* **46**, 685 (1972)
- [9] S. Martin and P. Kauffman, "A field and laboratory study of wave damping by grease ice," *J. Glaciology* **96**, 283 (1981)
- [10] K. Newyear and S. Martin, "A comparison of theory and laboratory measurements of wave propagation and attenuation in grease ice," *J. Geophys. Res.* **102**, 25091 (1997)
- [11] J.N. Newman, *Marine Hydrodynamics* (MIT Press, Cambridge MA, 1977)
- [12] G. DeCarolis, P. Olla and L. Pignagnoli, "Effective viscosity of grease ice in linearized gravity waves," *J. Fluid Mech.* **535**, 369 (2005)
- [13] C.W. Gardiner, *Handbook for stochastic methods*, third edition (Springer NY, 2004)
- [14] E.J. Hinch and L.G. Leal, "Constitutive equations in suspension mechanics. Part 2. Approximate forms of a suspension of rigid particles affected by Brownian rotations," *J. Fluid Mech.* **76**, 187 (1975)
- [15] C.M. Bender and S.A. Orszag, *Advanced mathematical methods for scientists and engineers* (McGraw-Hill, NY, 1978)